Hybrid particle swarm optimization-grey wolf optimizer algorithm for sidelobe reduction in radar communication

SARBJIT SINGH[1,*], SUMIT MALHOTRA[2], R. S. KALER[3], A. K. KOHLI[3]
[1]*Electronics & Communication Engineering Department, Chandigarh Engineering College, CGC-Landran, Mohali, India*
[2]*Computer Science and Engineering Department, Chandigarh University, Gharuan, Mohali, India*
[3]*Electronics & Communication Engineering Department, Thapar University, Patiala, Punjab, India*

Radar systems rely on effective sidelobe suppression to concentrate energy on the primary lobe, ensuring accurate target detection and minimizing false identifications. In both military and civilian applications, sidelobe reduction plays a crucial role in enhancing precision by mitigating clutter and environmental interference. Uncontrolled sidelobe allow unwanted reflections from structures, water surfaces, and terrain, introducing noise that degrades radar sensitivity. To address this, polyphase codes are optimized using a hybrid optimization algorithm that integrates particle swarm optimization (PSO) and the gray wolf optimizer (GWO). MATLAB was utilized in the simulative analysis and optimization process. This approach combines the global search efficiency of PSO with the local refinement capabilities of GWO, achieving superior sidelobe suppression while preserving resolution and detection accuracy. The proposed method enhances radar performance by reducing interference, improving target discrimination, and increasing resilience against jamming, making it a robust solution for modern radar applications. Optimization of P4 polyphase code using genetic algorithm yields a maximum signal-to-noise ratio of 21.91dB for Tukey window. On the other hand when the P4 polyphase codes are optimized using PSO and gray wolf algorithm then for Tukey window, signal-to-noise ratio of 31.78dB is achieved. Our results shows that hybrid algorithm performs better than the other algorithms in terms of signal quality.

(Received October 1, 2025; accepted April 8, 2026)

Keywords: Radar, Sidelobe, Genetic algorithm, PSO, Gray wolf

1. Introduction

Radar is an electromagnetic system which is used for sensing, detecting and locating the objects present in the ambience and determining its position and velocity using RF waves. Radar technology is critical in a number of industries, including aerospace, military, navigation, and air traffic control, thus these devices must change and adapt to meet the ever-changing needs of the technological world [1]. Radar warning receivers, electronic assault systems, and electronic support systems are some of the hazards that modern radar systems must contend with. Modern radar system uses low probability of interception (LPI) signals to survive. These LPI transmissions are usually continuous pulse compression signals that are hard for electronic intelligence (ELINT) equipment to intercept [2]. The most widely used LPI signal is the polyphase code radar signal (Frank, P1, P2, P3, and P4 codes), which are derived from step frequency modulated and linear frequency modulated signals. Polyphase codes possesses some of the advantages and key characterstics such as high range resolution, doppler tolerance, ease of digital implementation, and produces multiple parallel ridges in the time-frequency analysis [3]. In fact, these are the essential component of radar system design, widely employed for sidelobe suppression and improve detection accuracy, lowers interference, and boost system performance [4]. Unwanted signals can reach the radar receiver through sidelobes, which can cause problems including clutter, false alarms, and susceptibility to electronic countermeasures. Radars can concentrate more energy on the primary lobe by efficiently suppressing sidelobes, guaranteeing that detected signal comes from legitimate targets rather than from undesired sources. In both military and civilian radar applications, this increases the precision of target recognition and reduces the possibility of false target identification [5]. The capacity of sidelobe suppression to lessen clutter and environmental interference is also one of its main advantage. Sidelobes allow for the entry of reflections from buildings, water surfaces, and topography, which produces extra noise and lowers radar sensitivity. Reducing sidelobe levels improves the radar system's capacity to detect weak or far-off objects by helping it differentiate between real targets and background noise [6]. For applications where accurate target detection is required, such air traffic control, weather monitoring, and surveillance, this is especially important. The ability of sidelobe suppression to strengthen defense against electronic warfare and jamming is another significant benefit. Radar with high sidelobes are vulnerable to deliberate jamming, in which hostile forces send signals into the sidelobes to interfere with radar function [7]. The system is less vulnerable to electronic attacks when sidelobe levels are decreased, guaranteeing that it will continue to work even in hostile circumstances [8]. For military applications, where radar systems must function dependably in the face of hostile attempts to fool or disable them, this is particularly crucial.

Additionally, sidelobe suppression enhances target localization and tracking. Strong sidelobes can cause the radar system to pickup interference signals from undesirable directions, which can cause mistake in determining the position, velocity, and trajectory of a target. In applications where accurate tracking is crucial, such as missile guidance, air defense, and autonomous navigation, this could be an issue [9]. The radar can maintain precise and constant tracking by reducing sidelobe interference, which guarantees more dependable operations [10].

In radar systems like synthetic aperture radar (SAR) and inverse synthetic aperture radar (ISAR), sidelobe suppression is crucial for enhancing imaging quality in addition to tracking and detection. Unwanted sidelobe energy can cause distortions and abnormalities in radar images [11]. Radar systems can improve image resolution and contrast by using sidelobe reduction techniques like adaptive beam forming and windowing function [12]. This makes more useful for tasks like environmental monitoring, remote sensing, and reconnaissance [13]. Considering all things, it is true that sidelobe suppression is necessary to keep radar systems reliable and effective. In applications such as security, aviation, military, or meteorology, lowering sidelobe levels guarantees precise target identification, lessens susceptibility to interference, and improves overall operating effectiveness[14]. Modern radar systems can now attain greater precision and robustness against external threats because of the improvement in sidelobe suppression techniques. The main sidelobe suppression strategies employed in contemporary radar systems can be divided into three categories: time-domain techniques, frequency-domain techniques, optimization techniques and adaptive techniques. Time-domain methods reduce sidelobes and enhance radar performance by directly affecting time-domain signals [15]. Frequency domain methods suppress sidelobes by altering the radar signal's frequency spectrum [16]. To attain the best sidelobe suppression, optimization methods are utilized to adjust radar signal characteristics and antenna array topologies [17]. On the other hand adaptive method effectively suppresses the sidelobes by dynamically modifying the radar system parameters in response to current environmental conditions.

2. Literature review

Thakur et al. [18] used orthogonal polynomials to create sequences by adjusting the optimal parameter γ in order to simultaneously obtain a large bandwidth and few sidelobes. The polynomial orders that offer a greater bandwid that ideal γ value, are selected. To reduce sidelobes more effectively, the value of γ must be optimized. They have suggested the use of Chebyshev orthogonal polynomial (COP) and Legendre orthogonal polynomial (LOP) sequences for varying number of transmitting antennas in MIMO radar, to reduce peak sidelobe levels (PSL) and cross-correlation sidelobe levels (CCSL). Additionally, the performance of the developed sequences for synthetic aperture radar (SAR) imaging applications has been examined using the least square estimate (LSE) and capon estimate (CE) methodologies. Liu et al. [19] suggested a novel technique for sidelobe suppression that combines the SVA algorithm with the bidirectional recurrent neural network (BiRNN). BiRNN is used to extract the sidelobe and main lobe features of radar data, allowing for sidelobe suppression at any Nyquist sampling rate. The success of the BiRNN-SVA approach is confirmed by quantitatively evaluating the main lobe energy and the sidelobe suppression performance using the data from the land flight experiment of the fully polarized microwave scattero meter. The experimental finding shows that the BiRNN-SVA approach has better PSLR and ISLR than the GSVA and MSVA algorithms and can be used with data at any Nyquist sampling rate. More fine details and edge features are preserved in the image processed using the suggested method. In comparison to the GSVA algorithm and MSVA algorithm, the image contrast and focus have increased by31.6% and 3.6%, respectively, and by 4.4% and 1.1%. Also Fan et al. [20] suggested a digital guidance-based method to accurately detect the target's main and sidelobes, which is crucial for ship borne and measurement control radars. Zhang et al. [21] utilized a ground-based radar system with a low sidelobe array. One crucial thing to take into account is the sidelobe increase brought on by the radome. This paper presents an accurate method for estimating sidelobe increment due to spherical radomes. It compares simulation results with measured data and finds that the estimation of sidelobe increment of radomes on low sidelobe arrays can have a 90% confidence interval. For the design of high-performance radomes, it is particularly helpful.

Karamazov et al. [22] described the construction of asymmetric response signal compression and separation filters for multiple-input multiple-output (MIMO) radars that employ pulses longer than the maximum reflected signal return time. These radars exhibit a very strong stationary reflection in the zero-range due to direct transmission of the signal to the receiver. Liu et al. [23] suggested using the p-normas a correlation sidelobe performance metric and is represented by p-ISL. They have also discussed a p-MM algorithm based on the majorization- minimization (MM) framework to minimize the p-ISL. This technique reduces the difficult p-order polynomial minimization problem to a set of low-order easy optimization problems. The p-MM algorithm can successfully suppress the correlation sidelobe level and achieve a good balance between the PSL and ISL metrics, according to numerical data. Albagory et al. [24] discussed an efficient beam forming technique at the aggregator node in the patient wireless body area network, to improve the communication performance with the gateway node using C-shaped switched-beam antenna arrays. Also Albagory et al. [25] suggested an efficient self-reconfigurable spherical-cap antenna array and 3D beam forming technique for symmetrical beam patterns with low sidelobe and backlobe levels.

Moreover, Venkatamuni et al. [26] created the radar

waves according on the target's environmental factors, radar use, and target type to be identified. Dual band chirped hybrid waveforms with an enhanced main-to-sidelobe ratio are presented in this article. Novel waveforms with main-to-sidelobe ratio (MSLR) which is 24dB greater and exhibiting strong range resolution, were produced experimentally. They have achieved this performance without major lobe broadening, post-processing, and SNR loss.

Kislyy et al. [27] employed phased coded waveforms from satellite or aerial synthetic aperture radars (SARs) to obtain highly detailed images. SAR can produce high-resolution images with a high signal-to-noise ratio using this method. This method's primary drawback is its high sidelobe intensity, which becomes noticeable as rows of brilliant dashes, centered on a single or complex target response that is codirectional with the range axis. In essence, this impact lowers the quality of visual analysis of images by the human eye and significantly diminishes the capabilities of automatic image processing methods. Because of this, there are numerous approaches that lower sidelobe level while imposing varying trade-offs. The binary sequence's circular shift is one of these techniques. Every sequence that is emitted, is shifted cyclically, and with each shift, the autocorrelation function is accumulated. Finding the ideal circular shift parameter is essential for using this method effectively. The circular shift step or total number of autocorrelation function accumulations should be the primary parameter. The analytical study of sidelobe suppression caused by cyclic accumulation in the M-sequence autocorrelation function is presented in this paper.

In addition, Liao et al. [28] suggested a waveform design technique for random stepped frequency radars (RSFR)in order to attain ultra-low sidelobes in its high-resolution range profile (HRRP). The HRRP can be produced by synthesizing the wide-band using the randomly distributed modulated frequencies of RSFR. They have shown that by aligning the modulated frequency with the window type distribution, the HRRP sidelobes can be considerably reduced. Their simulation results shows that the suggested technique can attain a sidelobe level which is comparable to that of windowed linear stepped frequency radar, without reducing the output signal's power and likelihood of target detection is increased.

3. Research methodology

Modern radar systems must contend with some of the hazards such as radar warning receivers, electronic assault systems, and electronic support system. These radar systems uses the low probability of interception (LPI) signals to survive. These LPI transmissions are usually continuous pulse compression signals that are hard for electronic intelligence (ELINT) equipment to intercept. The most widely used LPI signals are the polyphase codes radar signals (Frank, P1, P2, P3, and P4 codes), which are derived from step frequency modulated and linear frequency modulated signals. They are extremely favored in LPI radar due to their high range resolution, Doppler tolerance, and ease of digital implementation. The sidelobe reduction filters utilizing windowing function are hybrid optimizing code and enhances the radar performance by carefully selecting the polyphaser code.

In this research, a hybrid optimization technique that combines the PSO and Gray Wolf algorithms is suggested. A new swarm intelligence system called Grey Wolf Optimization was developed based on the group hunting behavior and management hierarchy of grey wolves. The notion of this algorithm is very simple, need few parameters and programming is executed easily. Also distributed parallel computing and strong global search potentials are supported in this algorithm. Naturally, grey wolves are eager to animate in containers and follow a strict social hierarchy. A pack consisted of 4 kinds of wolves, and ranks are assigned to them from upper most to lower most in the social hierarchy: α wolf, β wolf, δ wolf, and ω wolf. Additionally, this algorithm relies on the predation behavior and social hierarchy of grey wolves. Its particular mathematical model is described as follows:

Surround the prey: The primary goal of the hunting process was to encircle the target. The main goal is to calculate the distance between the prey and the grey wolf at the moment and update the position based on that distance. Grey wolves' approach to encircling the target is described as follows [29]:

$$(t+1)=(t)-A\times D \tag{1}$$

$$D=|C\times(t)-X(t)| \tag{2}$$

In this, equation (1) denotes the updating process of location of grey wolf, and equation (2) illustrates a formula to compute the distance among grey wolves and their hunting target. The current iteration number is denoted with t, (t) is used to denote the existent locations of the target and (t) for wolf at t. A and C are employed for denoting coefficient vectors which are computed using equation (3) and equation (4) as [29]:

$$A=2\times a\times r_1-a, \tag{3}$$

$$C=2\times r_2, \tag{4}$$

$$a = 2 - 2 \times \frac{t}{t_{max}} \tag{5}$$

In this equation, a denotes the convergence factor, and a linear alleviation is found within range [2,0] after maximizing the number of iterations. r_1 and r_2 are employed random vector within range [0,1]. The equation (5) is used to define the computation formula for a and t_{max} is used to define the extreme number of iterations.

Hunting: A non-fixed search environment has not any specific place of optimal solution. For simulating the predatory strategy of grey wolves: α, β, and δ are considered which may have an enhanced awareness of the prey's likely position. The initial one is employed as an optimal solution, latter as the sub-optimal solution, and

last one as 3^{rd} optimal solution. Other Gray wolves are capable of modifying their places on the basis of α, β, and δ wolves, and their computation expressions are defined as [29]:

$$\begin{aligned} D_\alpha &= |C_1 \times X_\alpha - X(t)| \\ D_\beta &= |C_2 \times X_\beta - X(t)| \\ D_\delta &= |C_3 \times X_\delta - X(t)| \end{aligned} \quad (6)$$

$$\begin{aligned} X_1 &= |X_\alpha \times A_1 - D_\alpha| \\ X_2 &= |X_\beta \times A_2 - D_\beta| \\ X_3 &= |X_\alpha \times A_3 - D_\delta| \end{aligned} \quad (7)$$

$$X(t+1) = \frac{(X_1+X_2+X_3)}{3} \quad (8)$$

In these equations, D_α is employed to illustrate the distance amid current grey wolf and α wolf; D_β for the distance from current to β wolf; D_δ is used to define the distance amid current and δ wolf; and X_α is a position vector of α wolf, X_β is position vector of β wolf, and X_δ is position vector of δ wolf. (t) shows the current location of grey wolf. The random vectors are represented with C_1, C_2, and C_3 and equation (4) is executed to compute them. Equation 3 is executed to compute A_1, A_2, and A_3. In addition, the movement step size and direction of grey wolves in relation to α, β, and δ are determined using equation (7) and equation (8) is used as the position-updating expression used by grey wolf individuals. The PSO algorithm is planned in accordance with the particle behaviour, like flocking, swarming and herding. Every particle is capable of changing its flight based on the self or previous experience of flight of its companion. The place of food is known to it due to its own experience and identifies this location as personal best position with (P). Moreover, the particle is considered as the finest position in case a swarm is defined as global test position(G).The hybrid optimization algorithm is shown in Fig. 1. This algorithm aims to reconstruct this phenomenon for addressing the problems of real-time [5]. In addition, the particles are assisted in generating a swarm. These particles are useful to fly arbitrarily in the solution space at velocity v_i at position x_i and change their places relied on the personal experience, social and cognitive nature. The position and velocity of every particle i at tth generation are defined as [29]:

$$v_i(t+1) = wv_i + c_1r_1\big(P_i(t) - x_i(t)\big) + c_2r_2\big(G_i(t) - (x_i)\big) \quad (9)$$

$$x_i(t+1) = x_i(t) + v_i(t+1) \quad (10)$$

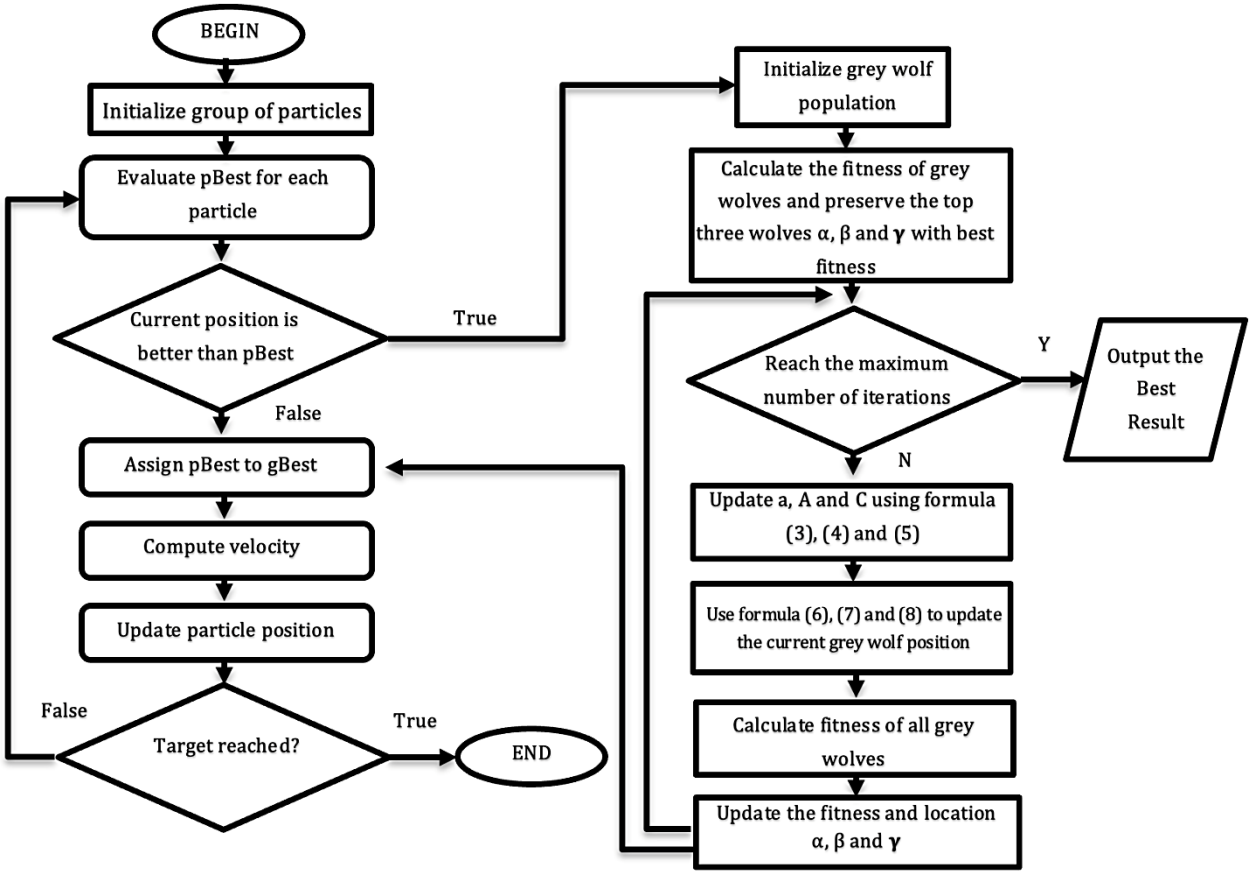

Fig. 1. Hybrid optimization algorithm

4. Results and discussions

This research work is based on the sidelobe suppression using polyphase codes. The P4 polyphase codes are used for the suspension of sidelobes. The results and discussion chapter is four phase which includes that in the first phase P4 polyphase codes are applied on the radar signal with various type of windows for the sidelobe suppression. In the second phase, genetic algorithm is applied on the P4 polyphase codes are get optimized for the suspension of sidelobe. In the third phase hybrid optimization algorithm which is the combination of PSO and Gray wolf algorithm are applied on P4 polyphase codes for the suspension of sidelobe. In the last section results of every phase is compared in terms of certain parameters. The various simulation parameters are considered which are described in the Table 1.

Table 1. Simulation parameters

Parameter Name	Value
Sampling Frequency, f_s	1e6Hz
Pulse Duration, T	1e-3s
Radar Signal Frequency, f_0	100e3Hz
Number of Samples	Sample Frequency* Pulse Duration
Window type	Kaiser, Hamming, Hanning, Blackman, Tukey

4.1. P4 Polyphase with windows for sidelobes suspension

The five windows are applied with the P4 polyphase codes for the suspension of sidelobes. The impact of each window on P4 poly phase codes are described in this section. Fig. 2(a) and 2(b) shows the impact of Kaiser and Hamming window with P4 polyphase codes for sidelobe suspension. Fig. 3(a) and 3(b) shows the impact of Blackman and Hanning window with P4 polyphase codes for sidelobe suspension. Fig. 4 shows the impact of Tukey window with P4 polyphase codes for sidelobe suspension.

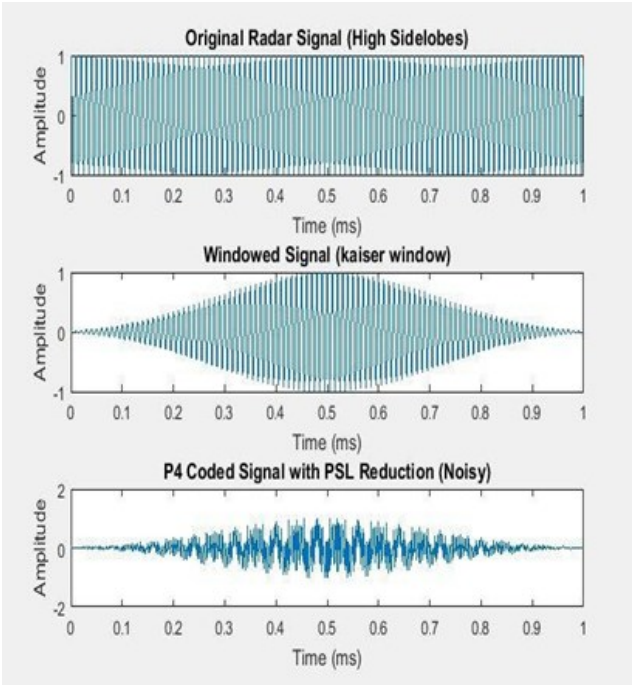

(a)

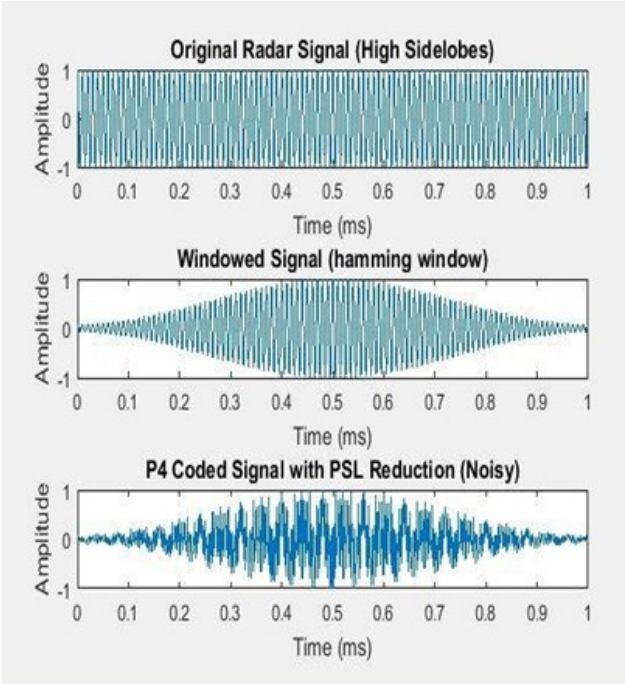

(b)

Fig. 2(a) Kaiser window with P4 codes and Fig. 2(b) Hamming window with P4 codes (colour online)

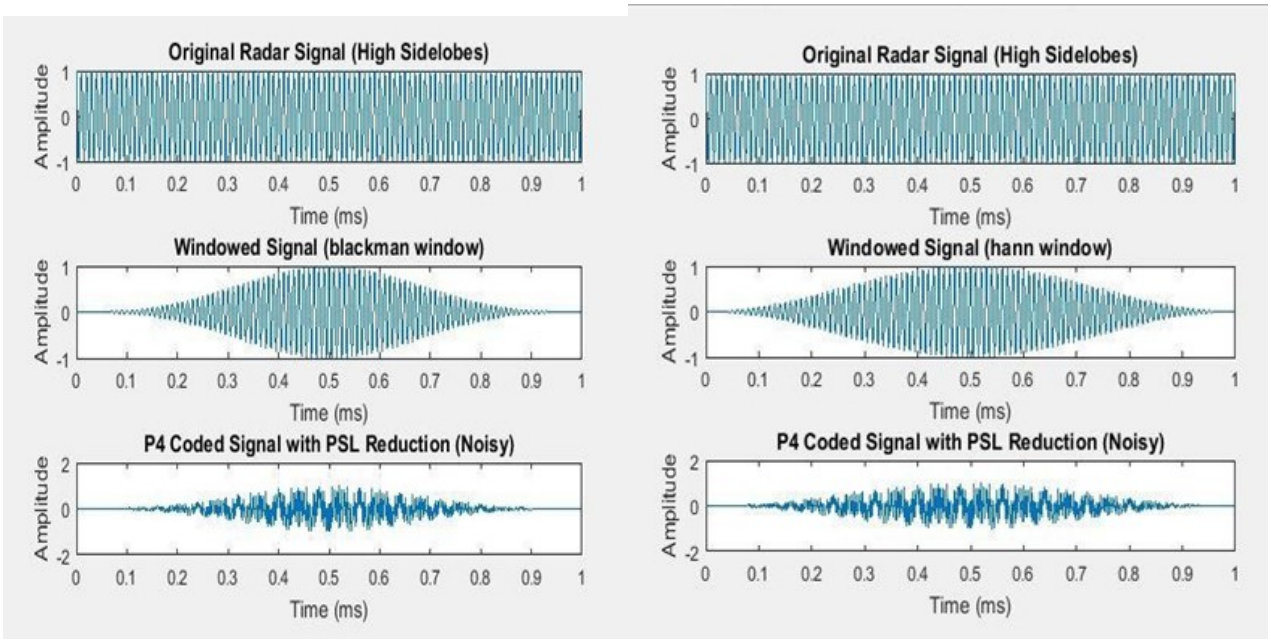

(a) (b)

Fig. 3(a) Blackman window with P4 codes and Fig. 3(b) Hanning window with P4 codes (colour online)

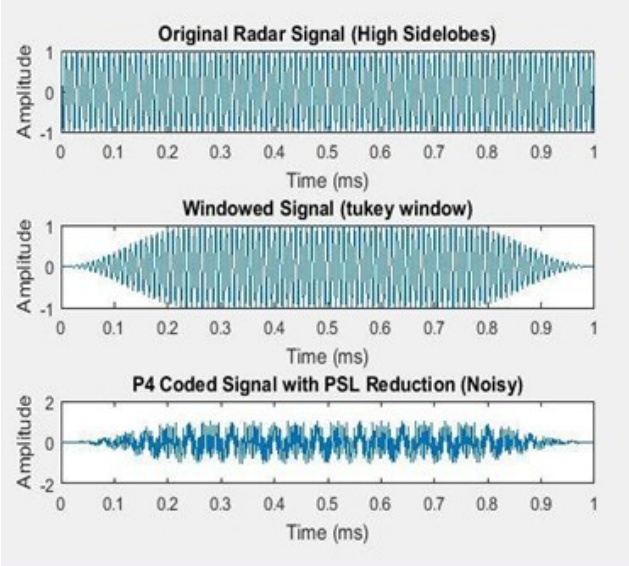

Fig. 4. Tukey window with P4 codes (colour online)

4.2. P4 Polyphase with genetic algorithm and windows for sidelobes suspension

The five windows are applied with the P4 polyphase genetic codes for the suspension of sidelobes. The impact of each window on P4 poly phase genetic codes are described in this section. Fig. 5(a) and 5(b) shows the impact of Kaiser and Hamming window with P4 polyphase genetic codes for sidelobe suspension. Fig. 6(a) and 6(b) shows the impact of Hanning and Blackman window with P4 polyphase genetic codes for sidelobe suspension. Fig. 7 shows the impact of Tukey window with P4 polyphase genetic codes for sidelobe suspension.

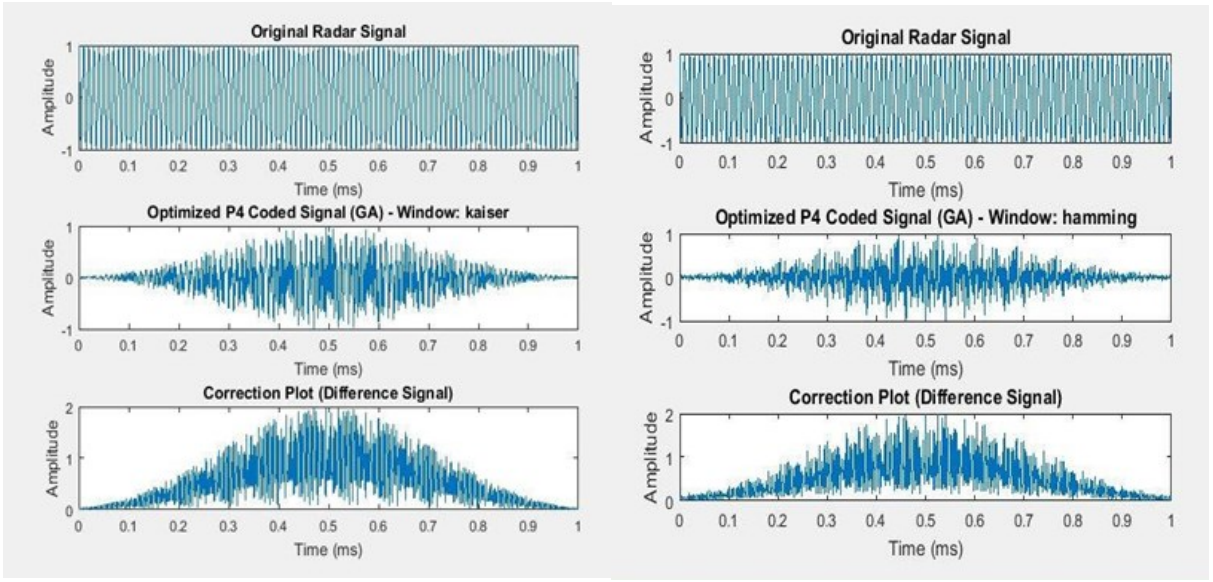

(a) (b)

Fig. 5(a) Kaiser window with P4 genetic codes and Fig. 5(b) Hamming window with P4 genetic codes (colour online)

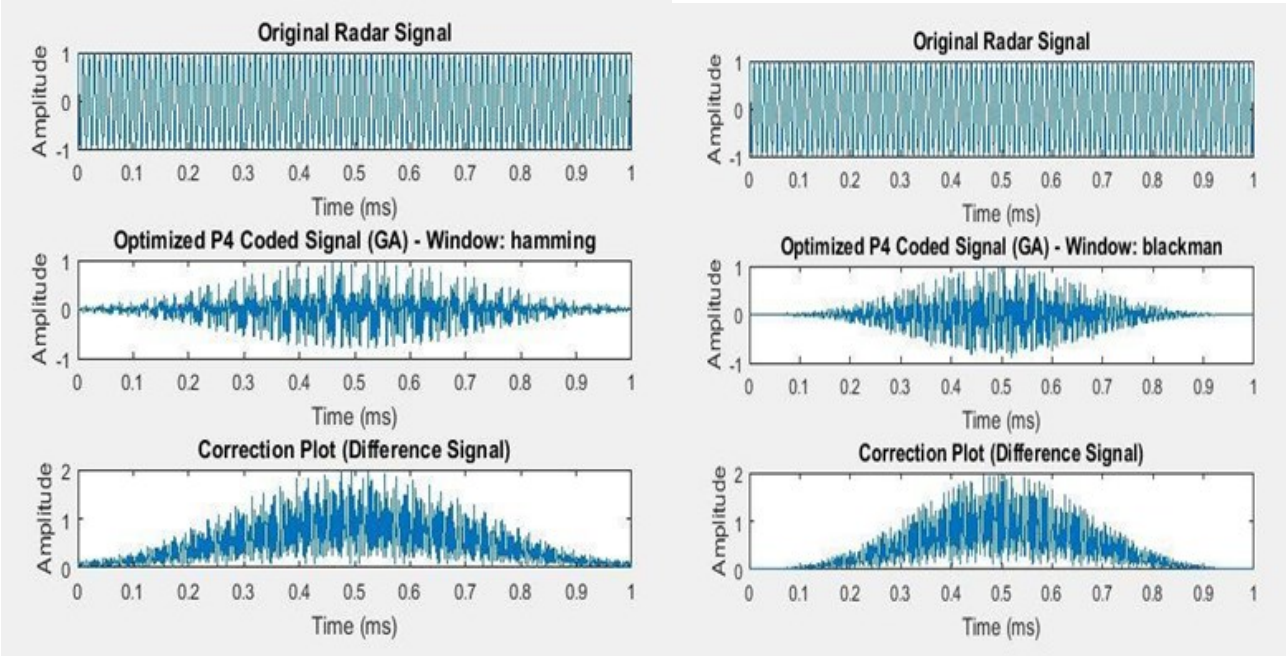

(a) (b)

Fig. 6(a) Hanning window with P4 genetic codes and Fig. 6(b) Blackman window with P4 genetic codes (colour online)

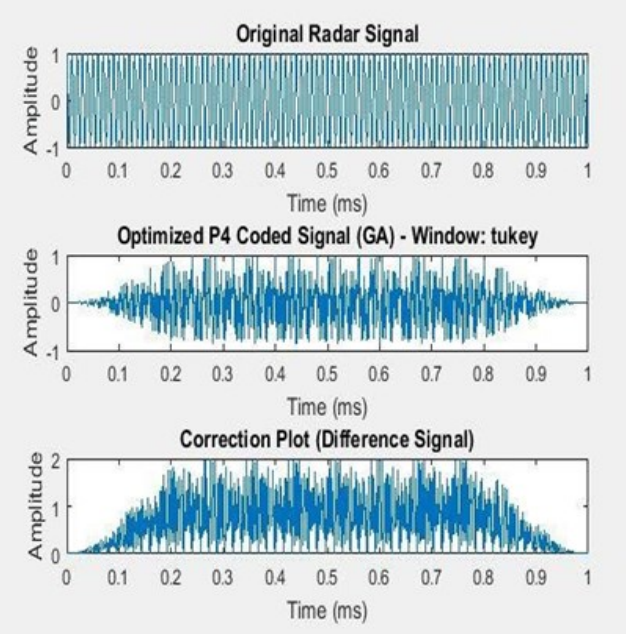

Fig. 7. Tukey window with P4 genetic codes (colour online)

4.3. P4 Polyphase with hybrid optimization algorithm and windows for sidelobes suspension

The five windows are applied with the P4 polyphase hybrid codes for the suspension of sidelobes. The impact of each window on P4 poly phase hybrid codes are described in this section. Fig. 8(a) and Fig. 8(b) shows the impact of Kaiser and Hamming window with P4 polyphase hybrid optimization codes for sidelobe suspension.

Fig. 9(a) and Fig. 9(b) shows the impact of Hanning and Blackman window with P4 polyphase hybrid optimization codes for sidelobe suspension. Fig. 10 shows the impact of Tukey window with P4 hybrid optimization codes.

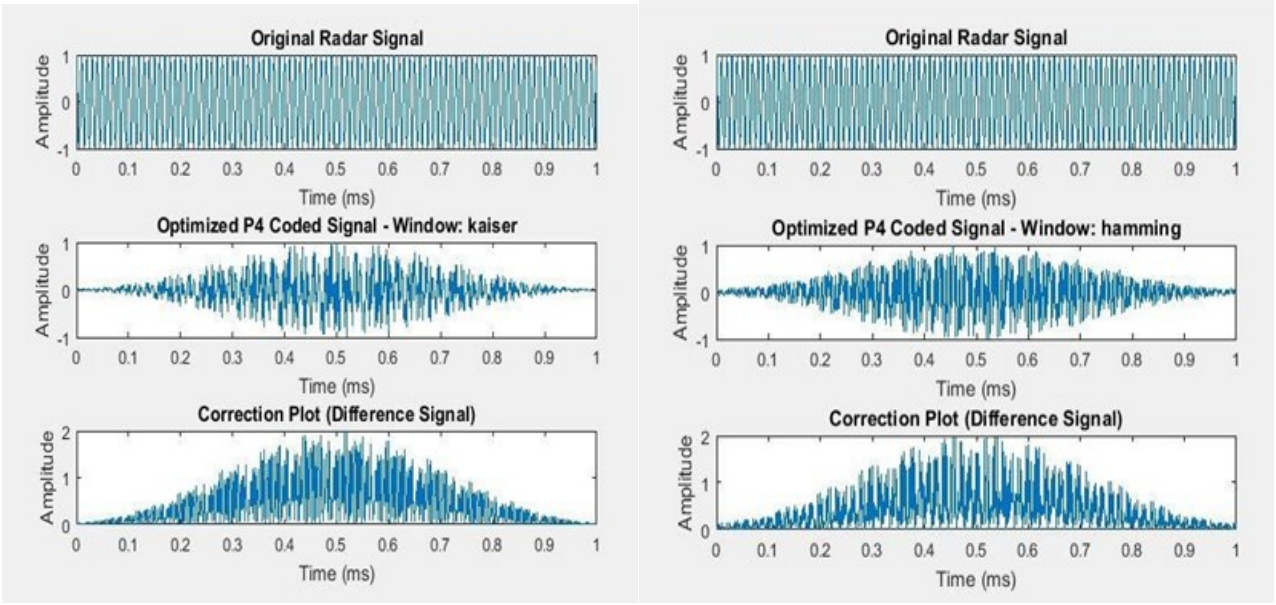

(a) (b)

Fig. 8(a) Kaiser window with P4 hybrid optimization codes and Fig. 8(b) Hamming window with P4 hybrid optimization codes (colour online)

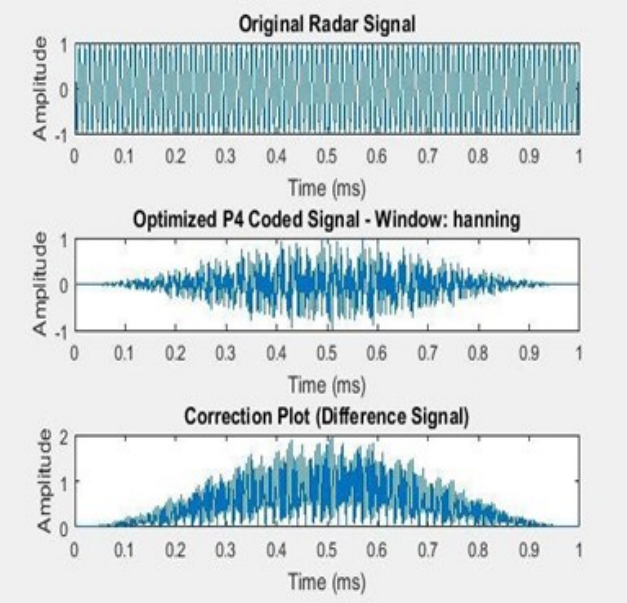

(a)

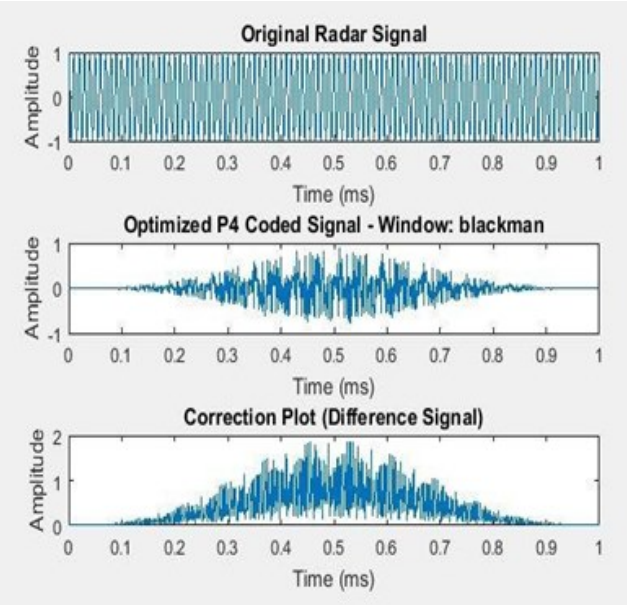

(b)

Fig. 9(a) Hanning window with P4 hybrid optimization codes and Fig. 9(b) Blackman window with P4 hybrid optimization codes (colour online)

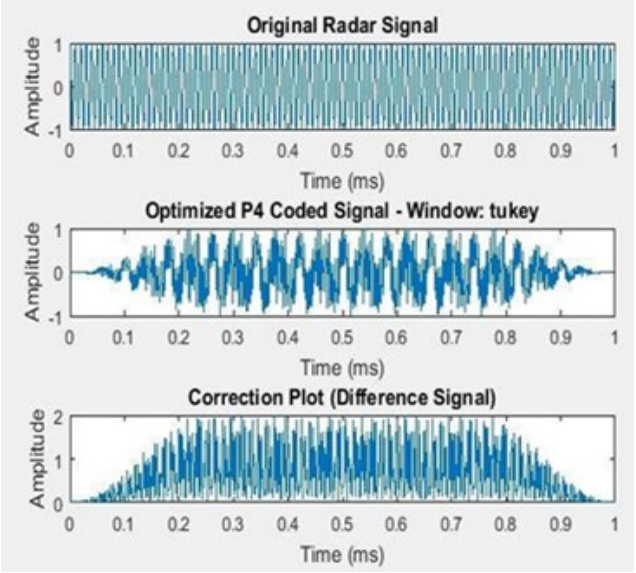

Fig. 10. Tukey window with P4 hybrid optimization codes (colour online)

5. Result comparison

In this research work, P4 polyphase coders are applied on the radar signals for sidelobe reduction. The three scenarios are discussed. In the first scenario, five windows are applied with the P4 polyphase code for sidelobe reduction. In the second scenario, five windows are applied with the P4 polyphase codes and results of P4 polyphase code are optimized using genetic algorithm. In the third and last scenario, five windows are applied with the P4 polyphase codes and results of P4 polyphase code are optimized using hybrid optimization algorithm which is the combination of PSO and Gray wolf algorithm. The results of the three scenarios are compared in terms of signal to noise ratio and these results are given in Table 2.

Table 2. Performance analysis

Window Name	P4 Polyphase code Non-optimized SNR(dB)	P4 Polyphase code with genetic algorithm SNR(dB)	P4 Polyphase code with PSO-GWO algorithm SNR(dB)
Kaiser	12.90	18.97	30.18
Hamming	11.12	17.89	29.89
Hanning	13.78	20.76	27.78
Blackman	16.89	18.90	28.56
Tukey	17.64	21.91	31.78

6. Conclusions

In this research, we have seen the impact of different windows with P4 polyphase hybrid optimization codes for sidelobe suspension. The proposed hybrid PSO-GWO algorithm for P4 polyphase code demonstrates excellent performance than the other algorithms in terms of minimizing sidelobe level and achieving a higher SNR for different windows while maintaining a reasonable computation time. Our results shows that the maximum achievable SNR with hybrid PSO-GWO algorithm for Kaiser, Hamming, Hanning, Blackman and Tukey window is 30.18dB, 29.89dB, 27.78dB, 28.56dB and 31.78dB respectively. This hybrid approach leverages the global exploration capabilities of PSO and the local exploitation efficiency of GWO, ensuring an optimal balance between exploration and convergence. By refining polyphase codes, the algorithm minimizes sidelobe levels while maintaining high resolution and detection accuracy. In future, the proposed hybrid PSO-GWO model can be further improved by using reinforcement learning.

Acknowledgements

I wish to acknowledge the Electronics and Communication Engineering Department at Chandigarh Engineering College, CGC-Landran, Mohali, Punjab, India for providing the resources and environment essential to conduct this research.

References

[1] J. Li, Z. Ma, L. Mao, Z. Wang, Y. Wang, H. Cai, X. Chen, Appl. Sci. **10**, 1207(2020).
[2] Y. Wang, W. Yang, J. Chen, H. Kuang, W. Liu, C. Li, Sensors **19**, 2764 (2019).
[3] M. Z. Hasan, H. Al-Rizzo, Sensors **20**, 2048 (2020).
[4] A. H. Nguyen, J. H. Cho, H. J. Bae, H. K. Sung, Photonics **7**, 20 (2020).
[5] K. Issa, H. Fathallah, M. A. Ashraf, H. Vettikalladi, S. Alshebeili, Electronics **8**, 1246 (2019).
[6] E. Juárez, M. A. Panduro, A. Reyna, D. H. Covarrubias, A. Mendez, E. Murillo, Symmetry **12**, 970 (2020).
[7] W. Choi, A. Georgiadis, M. M. Tentzeris, S. Kim, IEEE T. Antenn. Propag. **71**(2), 1437 (2023).
[8] Z. Qingwen, B. Zheng, Z. Yuhong, Journal of Electronics (China) **12**(1), 48 (1995).
[9] S. L. Wang, Z.-H. Xu, X. Liu, W. Dong, G. Wang, IEEE Sens. J. **18**(14), 5937 (2018).
[10] Z. Liang, Q. Liu, T. Long, IEEE T. Instrum. Meas. **69**(10), 7365 (2020).
[11] Z. Ding, J. Xie, B. Wang, H. Zhang, IEEE Access **8**, 177976 (2020).
[12] M. A. Richards, Fundamentals of Radar Signal Processing, New York, NY, USA: McGraw-Hill Education, 2014.
[13] V. Bhatia, S. Kaur, K. Sharma, P. Rattan, V. Jagota, M. A. Kemal, Wireless Communications and Mobile Computing **2021**, 2021513 (2021).
[14] K. Arora, J. Singh, Y. S. Randhawa, Wirel. Netw. **29**(6), 2437 (2023).
[15] D. Dhadwal, P. Sahni, V. Mittal, N. Agarwal, R. Mittal, Expert Systems with Applications **278**, 127231 (2025).
[16] Y. Xu, A. Wang, J. Xu, IEEE T. Aero. Elec. Sys. **58**(2), 834 (2022).
[17] W. Wei, X. Yu, Q. Lu, X. Wang, G. Cui, IEEE Signal Proc. Let. **30**, 284 (2023).
[18] A. Thakur, N. Garg, A. Thakur, D. S. Saini, AEU-International Journal of Electronics and Communications **193**, 155724 (2025).
[19] S. Liu, Y. Jia,Y. Liu, L. Zhai, X. Zhang, IEEE Journal of Selected Topics in Applied Earth Observations and Remote Sensing **17**, 1167 (2024).
[20] X. Fan, J. Hu, Y. Liu, X. Zhang, IEEE 3rd International Conference on Power, Electronics and Computer Applications (ICPECA), Shenyang, China, 925 (2023). https://doi.org/10.1109/ICPECA56706.2023.10075900.
[21] Q. Zhang, H. Sun, H. Zhou, S. Li, L. Wang, International Conference on Microwave and Millimeter Wave Technology (ICMMT), Qingdao, China, 1 (2023). https:// doi.org/10.1109/ICMMT58241.2023.10277263.
[22] S. Karamazov, P. Bezoušek, IEEE Access **11**, 48860 (2023).
[23] T. Liu, J. Sun, G. Wang, X. Du, W. Hu, IEEE Transactions on Aerospace and Electronic Systems **59**(4), 3797 (2023).
[24] Y. Albagory, AEU-International Journal of Electronics and Communications **123**, 153322 (2020).
[25] Y. Albagory, Wirel. Netw. **26**, 6111 (2020).
[26] T. Venkatamuni, S. Mandal, S. Kumar Sahoo, IEEE Microwaves, Antenna, and Propagation Conference (MAPCON), Bangalore, India, 1518 (2022). https://doi.org/10.1109/MAPCON56011.2022.10046708.
[27] S. A. Kislyy, I. A. Pchenikin, I. A. Kuzmin, M. S. Khasanov, E. L. Akashkin, K. S. Lyalin, IEEE International Multi-Conference on Engineering, Computer and Information Sciences (SIBIRCON), Yekaterinburg, Russian Federation, 2150 (2022). https://doi.org/10.1109/SIBIRCON56155.2022.10017030.
[28] Z. Liao, X. Yan, X. Hua, CIE International Conference on Radar (Radar), Haikou, Hainan, China, 1809(2021). https://doi.org/10.1109/Radar53847.2021.10028053.
[29] V. Kaur, A. Kaur Virk, Journal of Electrical System **20**(3), 7499 (2024).

*Corresponding author: singh.sb.optics@gmail.com